Article

Tribological Properties of Al$_2$O$_3$/Graphite-Al$_2$O$_3$ Laminated Composites under Water Lubrication Conditions

Zhengxian Di [1,2], Zhijia Wang [3], Xiaoyu Zhang [1,4], Jiaxin Si [3], Junjie Song [1,*], Hengzhong Fan [1], Yunfeng Su [1], Litian Hu [1] and Yongsheng Zhang [1,*]

[1] State Key Laboratory of Solid Lubrication, Lanzhou Institute of Chemical Physics, Chinese Academy of Sciences, Lanzhou 730030, China; dizhengxian@126.com (Z.D.); zhangxy605@163.com (X.Z.); hzhfan@licp.cas.cn (H.F.); yfsu@licp.cas.cn (Y.S.); lthu@licp.cas.cn (L.H.)

[2] Luoyang Institute of Science and Technology, Luoyang 471023, China

[3] Science and Technology on Helicopter Transmission Laboratory, Zhuzhou 412002, China; mrwangzhijia@126.com (Z.W.); heping@163.com (J.S.)

[4] Shandong Laboratory of Yantai Advanced Materials and Green Manufacturing, Yantai 264006, China

[*] Correspondence: songjunjie@licp.cas.cn (J.S.); zhysh@licp.cas.cn (Y.Z.); Tel.: +86-9314968833 (J.S.); Fax: +86-9314968019 (Y.Z.)

Abstract: High-performance Al$_2$O$_3$/graphite-Al$_2$O$_3$ laminated composites exhibit an excellent self-lubricating ability for moving components, such as sliding shaft sleeves and dynamic seals. The tribological behaviors of Al$_2$O$_3$/graphite-Al$_2$O$_3$ laminated composites should be studied extensively under water working conditions. Here, we attempted to explore the practicability of the Al$_2$O$_3$/graphite-Al$_2$O$_3$ laminated composite as a sealing material from a tribological point of view under water lubrication conditions. The tribological properties and mechanism of friction and wear of laminated composite ceramics were investigated under dry sliding friction, water environment, and suspended particle working conditions. It was found that the Al$_2$O$_3$/graphite-Al$_2$O$_3$ laminated composite has a better friction performance under water lubrication compared to dry sliding because of the separation effects formed by a water molecule film and a transfer film. Meanwhile, the wear rate under dry contact was found to be approximately six times that under water lubrication conditions. Under the water lubrication conditions, the formation of graphite films and water-adsorbed layers improved the anti-wear properties of the laminated materials, and the friction coefficient and the wear rate were as low as 0.16 and 1.76×10^{-6} mm^3/Nm, respectively. Under the suspended particle working condition, the solid particles destroyed the graphite lubricating film and abrasive wear dominated the wear mode. The Al$_2$O$_3$/graphite-Al$_2$O$_3$ laminated composite demonstrates a potential for application in dynamic sealing and sliding components.

Keywords: Al$_2$O$_3$/graphite composite; laminated structure; sliding wear; water lubrication conditions

1. Introduction

Wear failure is a common problem that leads to the functional failure of sealing devices and sliding shaft sleeves, which restricts the performance improvement of power and transmission systems significantly [1]. A dynamic sealing or sliding shaft sleeve component has a main friction surface and an auxiliary friction surface; the main friction surface needs to have a high bearing capacity and wear resistance, while the auxiliary friction surface needs to have a certain wear resistance. In addition, the working conditions of sealing devices and sliding shaft sleeves are becoming more and more harsh with the rapid development of components and involve multiple factors in interactive environments [2]. In a liquid rocket engine, the shaft face seal often works in liquid hydrogen or oxygen and needs to withstand ultra-low temperatures, requiring better friction and wear performance under liquid lubricating environments. These working conditions make the problem of wear resistance complex and place different requirements on the mechanical properties, tribological

properties, and service reliability of dynamic sealing and sliding shaft sleeve materials [3]. Deprez et al. used the Taguchi method to investigate the coefficient of dynamic friction and wear of dynamic sealing elements of carbon–silicon carbide tribological couples in water pumps of automotive combustion engines [4].

Graphite sealing technology, as a kind of high-speed dynamic sealing technology, is widely used, but the resistance of oxidation and the bearing capacity of graphite products are insufficient, which makes the sealing requirements of sealing devices difficult to attain under the condition of a higher load medium containing abrasive particles [5]. It is reported that NASA have tried to replace graphite sealing materials with self-lubricating composite ceramics, and relevant achievements have been applied in a few fields [6]. Stainless steel coated with diamond-like carbon film (DLC) or polymer is often employed for dynamic sealing under water lubrication. The DLC thickness determines the friction and wear rate, which gradually rises with the increase in the number of sliding cycles [7]. Water molecules can permeate the polymer superficial layer and cause volume swelling, resulting in structural instability, strength and hardness decrease, and wear increase [8]. Self-lubricating alumina ceramics have many excellent properties, such as high load bearing, wear resistance, high temperature resistance, and oxidation resistance [9,10]. Alumina ceramic-based self-lubricating materials can meet sealing requirements in harsh environments completely and do not increase the weight seriously [11].

Laminated composite materials are designed to enhance the mechanical properties of self-lubricating materials and can achieve the requirements for components [12]. The surface perpendicular to the layer direction has great wear resistance, and the surface parallel to the layer direction has a high bearing capacity, which is a good choice for the main friction surface and the auxiliary friction surface of a dynamic sealing material. Based on the above structural designation, Zhang et al. fabricated a series of alumina-based laminated self-lubricated ceramics [12–15]. The addition of heat-resistant Al_2O_3 in weak graphite can improve the interfacial bonding strength and the properties of the weak layer significantly [16]. Moreover, it can obstruct the oxygen transfer to inhibit the oxidation of graphite and furnish a good mechanical frame after graphite oxidation.

In our previous study, Al_2O_3/graphite-Al_2O_3 laminated composites showed impressive mechanical properties and interface stability [17]. However, the investigations on friction and the wear of Al_2O_3/graphite-Al_2O_3 laminated composites were focused on the structural design and performance under dry contact conditions [13,16,17]. Frictional heat and debris are mainly generated between the contact surfaces, and graphite is easily consumed during dry sliding conditions. Water, as a lubricant, can not only form a lubricating film to separate contact surfaces but also play a role in cooling [18]. Meanwhile, in hydropower plants and marine ships, dynamic sealing composite ceramic components are required to serve under water lubrication conditions. Applying Al_2O_3/graphite-Al_2O_3 laminated composites in such engineering areas, it is necessary to investigate the tribological behavior of these composites under such conditions. Up to now, the tribological performances of Al_2O_3/graphite-Al_2O_3 laminated composites have scarcely been reported under water lubrication conditions.

The tribological performances of ceramic composites under water lubrication conditions are quite different from those under dry contact conditions because they are dominated by the interactions between the ceramics and the water. The effect of water on the friction and wear of ceramic composites has three main aspects. Firstly, there is a lower friction coefficient under water lubrication conditions compared to dry contact conditions. Water has a boundary lubricating ability, so adsorbed layers can form to separate the contact of friction surfaces [19]. Additionally, lubricating water can reduce surface contact and decrease the shear force. Secondly, the wear rate for ceramic composites is lower under water lubrication compared to dry contact conditions [20]. Water has a cooling effect which can decrease work temperature. Zhao et. al. investigated friction and wear behaviors of different sealing materials under water-lubricated conditions and found that the pairing of metal-based graphite materials and diamond coating materials was a reasonable combi-

nation of sealing materials under both dry friction and water-lubricated conditions [21]. Thirdly, water has a low viscosity and a water-lubricating film is very thin [22] and can be easily destroyed, resulting in high friction or severe wear loss when solid–solid contact occurs in suspended and sediment particle environments. Briefly, water lubrication can change the tribological performances of ceramic composites. Thus, the tribological behavior and anti-wear mechanism of composites should be investigated under water and suspended or sediment particle environments.

In this study, Al_2O_3/graphite-Al_2O_3 laminated composites were used as the main research objects. The tribological properties and the mechanism of friction and wear in dry sliding, water, and sediment environments were investigated. The micro-structures of the surfaces normal and parallel to the lamination before and after friction were analyzed. The effects of lamination on the anti-wear and friction-reduction mechanisms were systemically investigated.

2. Materials and Methods

A schematic of the Al_2O_3/graphite-Al_2O_3 laminated composite is shown in Figure 1. The Al_2O_3 layer and the graphite-Al_2O_3 composite layer (the graphite content is 21.5 vol%) are marked as the A layer and the B layer, respectively. The thickness of the A layer is marked as d_A and that of the B layer is marked as d_B, where d_A and d_B are equal (265 μm) to alleviate the influence of changes in the layer thickness ratio and the residual stress between the different layers. The volume fraction (V_g) of the graphite phase in the total sample can be calculated using the following equation:

$$V_g = n_B \times V_B \times 21.5\% / [V_A \times n_A + V_B \times n_B] \tag{1}$$

where V_A is the volume of the individual Al_2O_3 layer, V_B is the volume of the individual composite layer modified by Al_2O_3, n_A is the number of A layers, and n_B is the number of B layers.
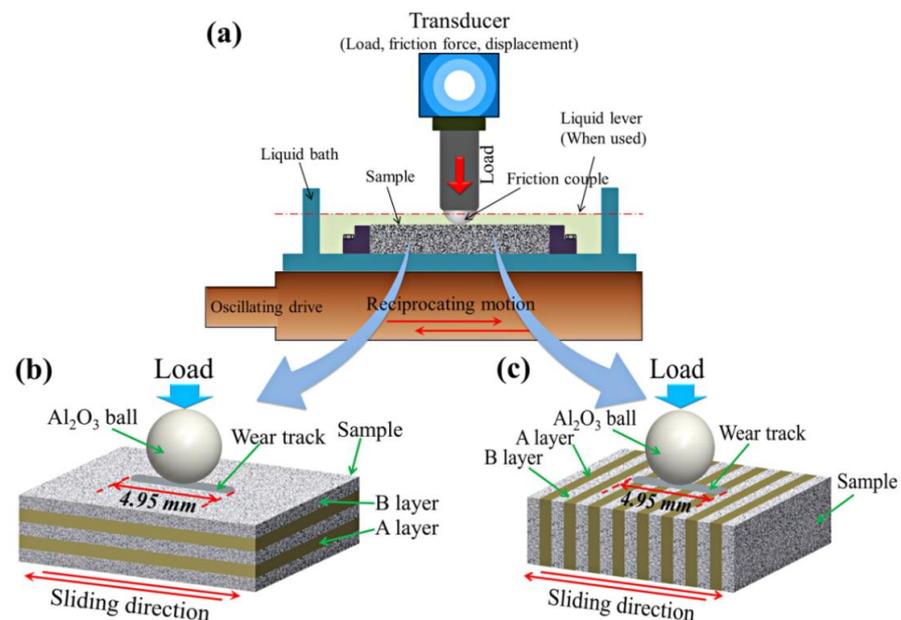

Figure 1. Schematic of friction tests on the different surfaces of Al_2O_3/graphite-Al_2O_3 laminated composites. (**a**) is a diagram of the friction experimental equipment, (**b**) is a schematic diagram of the friction test parallel to the layer direction, and (**c**) is a schematic diagram of the friction test perpendicular to the layer direction.

Commercial colloidal graphite powder (≤4 μm) and Al_2O_3 powder (80~200 nm) were used as raw materials, and 5 wt% TiO_2-CuO (TiO_2:CuO = 4:1) powder was used as a sintering aid. The detailed steps are as follows [12]: (1) ball milling by the dry mixing

method; (2) alternating stacking of A layers and B layers in a steel mold; (3) dry pressing and gain of green bodies; and, lastly, (4) hot pressing sintering in a graphite mold. Laminated composites were prepared with the same layer thicknesses (approximately 265 μm) and alternating stacking of graphite-Al_2O_3 composition powders and Al_2O_3 powders, with the graphite-Al_2O_3 composition powder content being 78.5 vol% Al_2O_3 and the graphite content being 21.5 vol%. The laminated composites were dry pressed at 180 MPa for 5 min, then hot pressed at 1400 °C and 25 MPa in an argon atmosphere for 120 min.

To simulate the environments of lubricating bushings in hydropower plants and marine ships, three test conditions were employed, which were expected to engender sliding against lightweight ceramics. In atmospheric environments with approximately 20% relative humidity, a deionized water environment and a water environment containing 5 wt% SiO_2 solid particles with a particle size of less than 1 μm were selected (before the experiment, the water and SiO_2 particles were ultrasonically mixed for 15 min). Friction tests were conducted on a standard UMT friction device (UMT-3MT, CETR, San Jose, CA, USA) in a reciprocating sliding condition at room temperature (20 ± 2 °C). The specimens were mated to Al_2O_3 balls 10 mm in diameter with 16 ± 0.5 GPa Vickers hardness and 0.04 μm surface roughness (Ra). The sample size for the friction tests was 12.5 mm × 12.5 mm × 4 mm.

Figure 1 shows the schematic of the contact configuration for the tests. The sliding directions were perpendicular/parallel to the laminar direction. The samples oscillated with a linear stroke of 4.95 mm at a constant frequency of 5 Hz for 3600 s. The tribological tests were performed at a constant pressure of 35 N (the pressure was based on the applied load and the contact area of the worn surfaces of the Al_2O_3 balls after the friction tests). Before the tests, the specimens were carefully polished to obtain a surface roughness of 0.1~0.3 μm (Ra) and then ultrasonically cleaned in acetone. All friction tests were carried out at least three times under the same conditions, and average values were obtained. The micro-morphologies and chemical compositions of the worn surfaces were analyzed using scanning electron microscopy (SEM; JSM-5600LV, JEOL, Tokyo, Japan), 3D surface profiling (MicroXAM-800, KLA-Tencor, Milpitas, CA, USA), and energy-dispersive spectrometry (EDS; JSM-5600LV, JEOL, Tokyo, Japan). The hardness of the specimens was measured by a micro-hardness tester (a square conical diamond indenter with an included angle of 136° on the opposite surface with a load of 0.5 kg). The wear rate (k) was calculated using the following formula:

$$k = A/(2 \times P \times f \times t) \tag{2}$$

where A is the area of the topography profile of a worn surface determined by a stylus profile meter, P is the applied load, f is the sliding frequency, and t is the total sliding time. The laminated composite ceramics in the water conditions were pinned under the deionized water, as shown in Figure 1.

Figure 2a shows the SEM images of the SiO_2 particles; the particle sizes are less than 100 nm, and the particle shapes are nearly spherical. Figure 2b shows the dispersion stability of a suspension with a solid content of 5 wt% SiO_2. SiO_2 particles and water were ultrasonically mixed for 15 min, forming a colloidal suspension. The suspension showed great dispersion stability after standing for 1 day, 14 days, and 27 days, and only a small amount of supernatant appeared near the upper surface after standing for 27 days. At last, a suspension containing 5wt% SiO_2 particles prepared for 1 day was employed to simulate the working environment of sand and gravel.
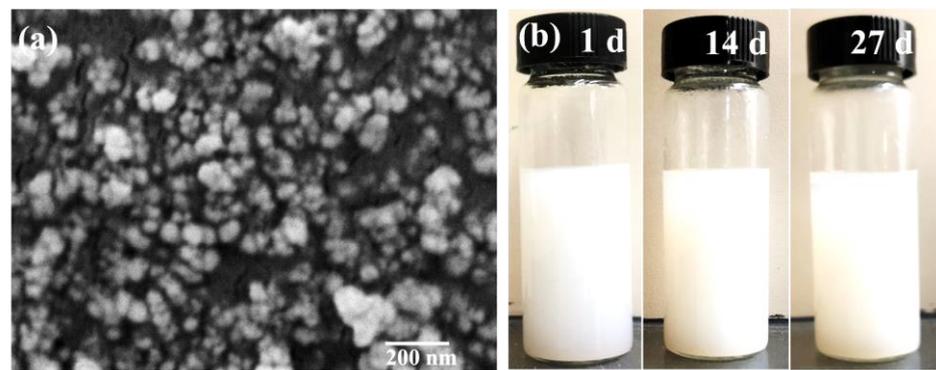
Figure 2. Micro-morphology of SiO$_2$ particles (**a**) and sediment experiment of suspension with 5 wt% SiO$_2$ particles (**b**).

3. Results

3.1. The Microstructures of the Laminated Composites

Figure 3 shows the optical images and micro-morphologies of the sintered Al$_2$O$_3$/ graphite-Al$_2$O$_3$ laminated composites. Figure 3a shows the surface perpendicular to the layer direction, which is an alternate arrangement of the Al$_2$O$_3$ layer (the A layer) and the graphite-Al$_2$O$_3$ composite layer (the B layer), and the laminates are relatively flat with a uniform thickness. Among them, the Al$_2$O$_3$ layers have a very dense microstructure, while the graphite-Al$_2$O$_3$ composite layers have some pores because the lamellar graphite is not easily compacted. The interlayer interface is relatively flat, without cracks, as shown in Figure 3b. Figure 3c shows the surface of a graphite-Al$_2$O$_3$ composite parallel to the layer direction, and a magnification is shown in Figure 3d, where the alumina particles are embedded in sheet-like graphite that has a porous structure. The typical laminated structure endows each surface with some merits in terms of friction and wear properties.
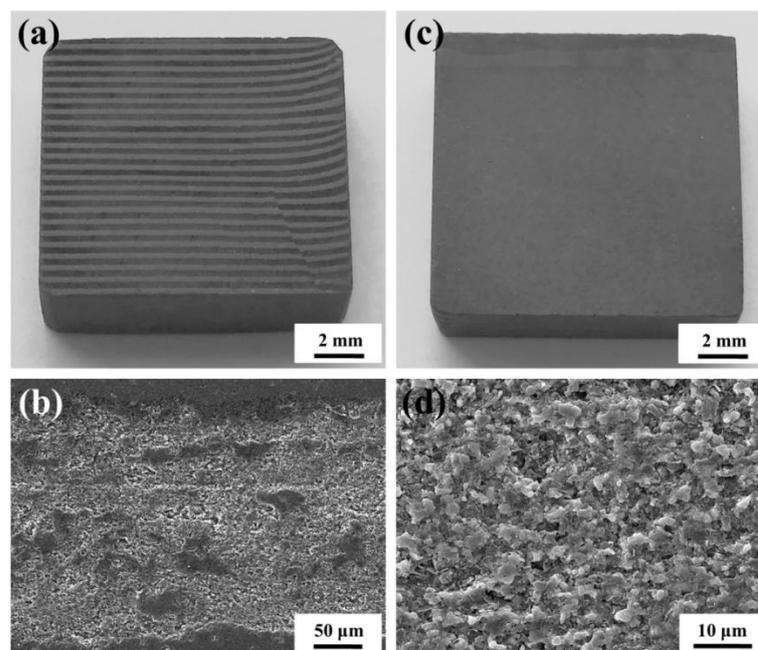

Figure 3. Optical and SEM microscopies of different surfaces of Al$_2$O$_3$/graphite-Al$_2$O$_3$ laminated composites: macrostructure (**a**,**c**) and microstructure of graphite-Al$_2$O$_3$ layers (**b**,**d**).

3.2. The Tribological Properties of the Laminated Composites

Figure 4 shows the friction coefficient curves of different surfaces of the Al$_2$O$_3$/ graphite-Al$_2$O$_3$ laminated composites under dry sliding friction, the water condition, and

water with 5 wt% SiO_2 particles. Under the dry sliding condition shown in Figure 4a, the friction coefficient of the Al_2O_3/graphite-Al_2O_3 laminated composites parallel to the layer direction is between 0.30 and 0.40, and the values show a certain fluctuation, while the composites perpendicular to the layer direction are more stable, with values between 0.28 and 0.32. Remarkably, the friction coefficients of the laminated composites decreased evidently when friction pairs were placed in the water conditions, as shown in Figure 4b. The friction coefficients of the surface parallel to the layer direction decreased to 0.10~0.20 but fluctuated apparently during the friction process, while they decreased to 0.15~0.16 for the surface perpendicular to the layer direction and became pretty stable after the running-in period. After adding 5 wt% SiO_2 particles into the water (in Figure 4c), the friction coefficients of the Al_2O_3/graphite-Al_2O_3 laminated composites increased and showed no evident fluctuation compared to the water condition without particles. The friction coefficients of the surface parallel to the layer direction increased to 0.21~0.22, while the friction coefficients of the surface perpendicular to the layer direction increased to 0.19 and became stable after the running-in period.
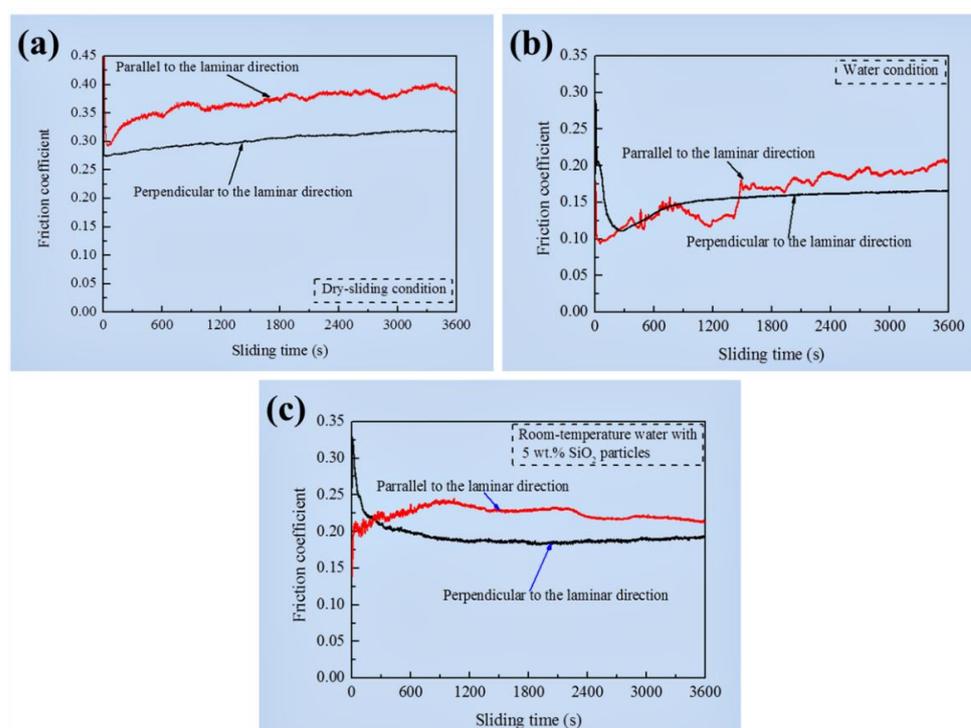

Figure 4. The friction coefficients for the different surfaces of Al_2O_3/graphite-Al_2O_3 laminated composites under different conditions: (**a**) dry sliding condition, (**b**) water condition, and (**c**) water with 5 wt% SiO_2 particles condition.

Figure 5 shows the wear rates of different surfaces of the Al_2O_3/graphite-Al_2O_3 laminated composites under the different conditions. The wear rates of the laminated composites under the water conditions are lower compared to the dry sliding friction condition. The solid particles in the water increased the wear rates of the laminated composites severely. In addition, compared to the surfaces parallel to the layer direction, the wear rate perpendicular to the layer direction decreases by orders of magnitude. Especially under water conditions, the wear rate perpendicular to the layer direction can be as low as 1.76×10^{-6} mm^3/Nm, which is two orders of magnitude lower than that parallel to the layer direction under the same condition.

Briefly, the friction coefficients of the Al_2O_3/graphite-Al_2O_3 laminated composites under the water conditions with or without suspended particles were lower than those under dry sliding friction, and the friction coefficients of the surfaces perpendicular to the layer direction were lower and more stable than those parallel to the layer direction. This

demonstrates that the test conditions and the configuration of the laminated composites had a great influence on the friction and wear properties.
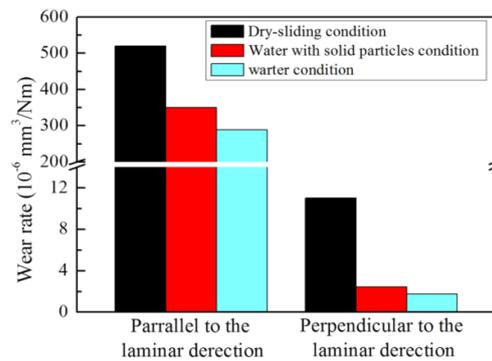

Figure 5. The wear rates of the different surfaces of Al_2O_3/graphite-Al_2O_3 laminated composites under different friction conditions.

From our previous research results [16], a comparison of the tribological performance of different alumina-based ceramics under dry sliding and water lubrication conditions is presented in Figure 6. The friction coefficient of the monolithic Al_2O_3 ceramic under dry sliding is 0.72, as shown in Figure 6a, and it approximately decreases by 50% after introducing graphite as a lubricant. The friction coefficients of the Al_2O_3/graphite-Al_2O_3 laminated composites are the lowest under both conditions. Figure 6b shows the wear rate of the alumina-based ceramics; the graphite-Al_2O_3 composite has the highest wear rate among all the ceramics under the dry sliding and water conditions. The Al_2O_3/graphite-Al_2O_3 laminated composites almost have the lowest wear rate among the four ceramics. Therefore, the Al_2O_3/graphite-Al_2O_3 laminated composites show preferable tribological properties under the dry friction and water conditions. In the preparation and application of seals, the Al_2O_3/graphite-Al_2O_3 laminated composites can tolerate a certain load and high temperatures. The surface perpendicular to the layer direction, as the main working surface, can exhibit better friction and wear performance under dry sliding friction, water, and suspended particle conditions, and it can also reduce the energy loss during work and improve the service life of components.
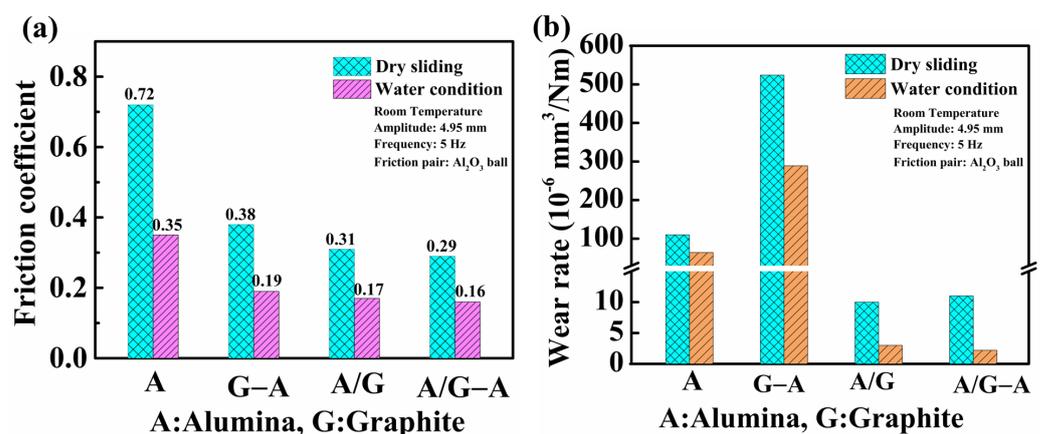

Figure 6. The friction coefficients (**a**) and wear rates (**b**) of different alumina-based ceramics under dry sliding and water conditions, where A is alumina, G-A is the graphite-Al_2O_3 composite, A/G is the Al_2O_3/graphite laminated composite, and A/G-A is the Al_2O_3/graphite-Al_2O_3 laminated composite.

3.3. Mechanism of Friction and Wear

The above results indicate that the surfaces of the Al_2O_3/graphite-Al_2O_3 laminated composites perpendicular to the layer direction show better wear resistance than those parallel to the layer direction under the three different working conditions. This can be attributed to the laminated composites with strong/weak layers that effectively improve the bearing capacity and wear resistance of composites by virtue of the high strength and anti-wear ceramic matrix layer. Typically, the layered structure reduces the low reliability caused by the high friction and inherent brittleness of Al_2O_3 under dry friction conditions and overcomes the weaknesses of the low bearing capacity, insufficient heat resistance, and wear resistance of graphite. In this way, the vulnerability from inadequate mechanical and tribological properties of conventional ceramic materials can be reduced, and the unification of mechanical properties and lubricating functions of ceramic materials can be realized. For graphite-Al_2O_3 composite ceramics (the B layer), the friction coefficient can be significantly reduced, but the wear rate will increase, unfortunately. The introduction of the graphite phase will form an interphase and destroy the continuity of the Al_2O_3 matrix, so that the mechanical properties of the composite ceramics, such as strength and hardness, will decline, reducing the crack resistance and the reliability of graphite-Al_2O_3 composite ceramics, as shown in Figure 6b.

Moreover, the Al_2O_3/graphite-Al_2O_3 laminated composite is apt to form lubricating films and transfer films compared with the graphite-Al_2O_3 composite ceramic. In the process of friction and sliding, the soft layers of graphite were subjected to extrusion of friction and thermal expansion, which was continuously transported to the laminated composite surface perpendicular to the layer direction and formed a relatively stable lubricating film [23]. And it continuously supplemented and provided a lubricating medium to form a "self-healing" effect, repairing the torn lubrication film during the friction process, inhibiting the laminated composite's directly contacting the friction pair. As a result, the surface of the Al_2O_3/graphite-Al_2O_3 laminated composite perpendicular to the layer direction under the three different working conditions showed better self-lubricating performance than that parallel to the layer direction, and the friction coefficient curves were more stable. For graphite-Al_2O_3 composite ceramics, a friction lubrication film was formed through wear and self-consumption. The hard Al_2O_3 phase underwent abrasive wear, aggravating the self-consumption of the graphite-Al_2O_3 composite ceramics.

In water working conditions, the bearing capacity of water is low owing to the low viscosity of the liquid. In an ab initio molecular dynamics study, Hass et al. revealed that the dissociative adsorption of water was energetically favored on an Al-terminated (0001) α-Al_2O_3 surface compared to molecular physisorption [24]. The surface of Al_2O_3 can form an electric double layer between the solid–liquid interface, which is composed of several dissociative adsorptions of water molecules about several nanometers in thickness away from the solid surface. This makes the electric viscosity of water increase exponentially, increasing the bearing capacity of water [25,26]. Furthermore, the water molecules on the solid surface are layered and directionally arranged; the molecules in the same layer maintain an independent integrity, and it is easy for sliding to occur between the layers. When a slip occurs, a shear plane with a certain potential is generated in the electric double layer, which provides a low shear resistance interface. In addition, the two friction surfaces were separated by the adsorption film; the layer adsorbed at the surface promoted the easy removal of the alumina debris [27], causing the friction coefficient to decrease and avoiding surface adhesion.

On the other hand, if graphite is exposed to air for a long time, its surface adsorbs hydrocarbon pollutants in the environment and becomes hydrophobic, while the newly formed surface is hydrophilic [28]. The water molecules will be arranged regularly near the graphite surface, and the rank density is high to form an obvious stable adsorption layer; the arrangement of water molecules is gradually disordered away from the graphite surface, and the density gradually decreases, forming a diffusion adsorption layer. Unfortunately, simulations show that the interaction between water and graphite is weak compared to

that among water molecules [29]. The adsorbed layer on the graphite surface can be easily destroyed by friction. This leads to expansion between graphite layers and decreases the shear resistance of graphite layers, resulting in better self-lubrication for graphite. In short, in water working conditions, the alumina plays an important part in boundary lubrication, the graphite is indispensable for self-lubrication, and the different lubrication mechanisms lead to different friction and wear behaviors compared to dry sliding conditions.

For the graphite-Al_2O_3 composite ceramic, the boundary lubrication of alumina is destroyed and presents discontinuity caused by the introduction of graphite; it exhibits an unstable friction coefficient parallel to the layer direction during sliding (Figure 4b). For the Al_2O_3/graphite-Al_2O_3 laminated composites perpendicular to the layer direction, the reduction in the friction coefficient is affected by the layered structure between the alumina and the graphite–alumina. Besides the lubrication film formed by graphite during sliding friction, water can form a certain fluid lubrication film on the friction surface (Figure 7c) during friction and sliding processes [30]. Moreover, the layer distance of the graphite is higher by one order of magnitude than the size of the water molecules, and the water molecules can diffuse into the graphite layer easily. Then, the distance between graphite layers increases by swelling from water molecule adsorption, which decreases the shear resistance of graphite layers and provides graphite with a better self-lubricating performance [31]. Thus, the friction coefficients of the alumina-based composite are low under the water lubrication conditions in Figure 6a. In addition, due to the periodic arrangement of the Al_2O_3 layer (the A layer) and the graphite-Al_2O_3 composite layer (the B layer), the B layer also contains 78.5 vol% of alumina; the high content of Al_2O_3 means that boundary lubrication plays a relatively stable role, and the friction coefficient is relatively stable accordingly. Furthermore, water can wash away the debris generated on the friction surface with the movement of the sample (Figure 7b), decreasing the hard particles and preventing abrasive wear from the friction pairs. Therefore, the Al_2O_3/graphite-Al_2O_3 composites perpendicular to the layer direction have lower friction coefficients in water working conditions than the graphite-Al_2O_3 composite ceramic.
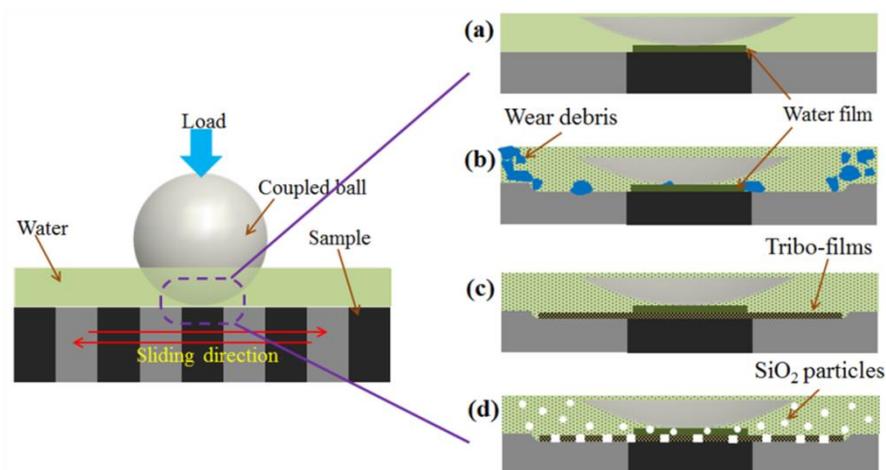

Figure 7. Schematic diagram of friction and wear mode under water working conditions. Al_2O_3/graphite-Al_2O_3 laminated composites perpendicular to the layer direction under water working conditions. (**a**) refers to placing the friction specimen under water lubrication conditions, and an adsorbed water film forms on the surface; (**b**) is for alumina undergoes abrasive wear and was washed away during the friction process; (**c**) refers to a graphite lubricating film formed on the surface of composite ceramics as friction progresses, on which was a water lubricating film; (**d**) is the destruction of two types of lubricating films by SiO_2 particles.

During the tests in the suspended particle conditions, the adsorptive water layer on the surface of the alumina was easily destroyed by SiO_2 particles in the water, and the shear lubrication of water decreased. Additionally, the SiO_2 particles increased abrasive wear in

the sliding process and tore the lubricating film on the graphite surface (Figure 7d) and also aggravated the friction and wear of the Al_2O_3/graphite-Al_2O_3 laminated composites. Thus, the friction coefficient and wear rates of the Al_2O_3/graphite-Al_2O_3 laminated composites in water containing SiO_2 particles were higher than those in pure water.

3.4. Friction and Wear Surface Analysis

The surface morphologies for the wear surfaces of the Al_2O_3/graphite-Al_2O_3 laminated composites under water working conditions are shown in Figure 8. The width of the worn surfaces is approximately 800 μm. Obviously, the addition of SiO_2 suspended particles makes the worn surface of Al_2O_3 (the A layer) become clearer and smoother and that of graphite-Al_2O_3 composites (the B layer) become rougher, as shown in Figure 8a. Without SiO_2 particles, a continuous graphite lubricating film forms on the surface of the Al_2O_3/graphite-Al_2O_3 composites, as shown in Figure 8c. Additionally, it can be seen that abrasive particles are generated and that steps appear at the interface between the A layer and the B layer of the Al_2O_3/graphite-Al_2O_3 laminated composites in the water working conditions with suspended SiO_2 particles (seen in Figure 8b); spallation occurs on the wear surface of the Al_2O_3 (the A layer), and the wear of the graphite-Al_2O_3 composites (the B layer) is serious. For the water condition without SiO_2 particles, the worn interface between the A layer and the B layer is relatively smooth, and the B layer has some large pores on the surface (Figure 8d).
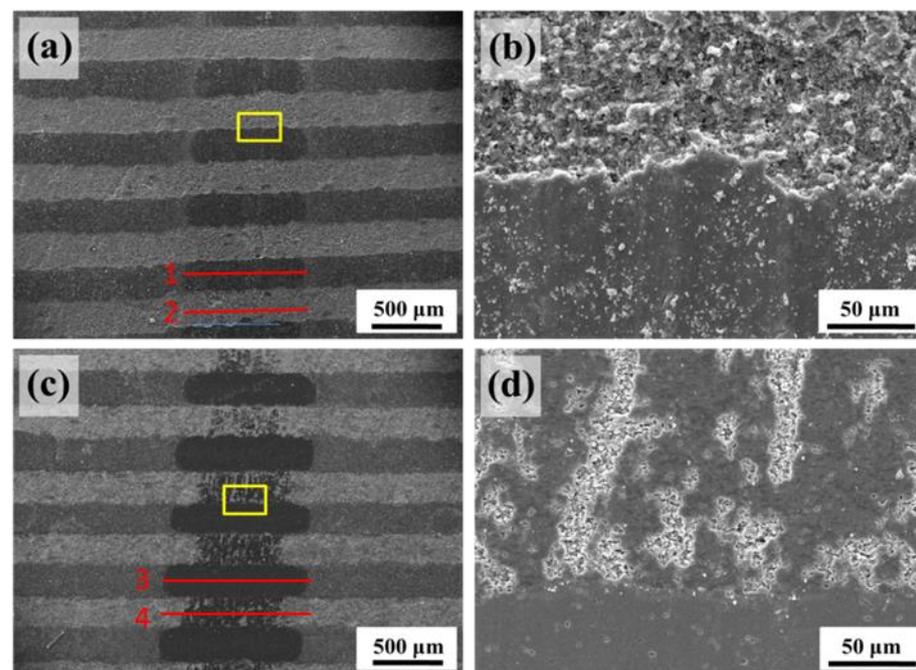

Figure 8. Worn surfaces and interface of Al_2O_3/graphite-Al_2O_3 laminated composites under water working conditions with SiO_2 particles (**a**,**b**) and without SiO_2 particles (**c**,**d**). Where line 1 and line 3 are on layer A, line 2 and line 4 are on layer B.

The micro-morphologies of the wear surfaces of the Al_2O_3/graphite-Al_2O_3 laminated composites perpendicular to the layer direction are shown in Figure 9. Figure 9a shows the micro-morphology of Al_2O_3 (the A layer), where the surface is relatively smooth with some pores, and the relative density is high. Figure 9d shows the morphology of the graphite-Al_2O_3 composites (the B layer), where the surface has some holes and graphite flakes are mixed with alumina grains, forming a relatively loose structure. Comparing the layers of the Al_2O_3/graphite-Al_2O_3 laminated composites under water working conditions with SiO_2 particles, numerous alumina abrasive particles were attached to the worn surface (Figure 9b) and the graphite was full of pores, and the worn surface of the B layer (Figure 9e)

was full of graphite debris and pores after the graphite was peeled off. Furthermore, there were some finer pores in the A layer, which were caused by shearing and peeling of Al_2O_3 particles that were not strongly bound during friction. Figure 9f shows the pores left after the peeling of graphite.
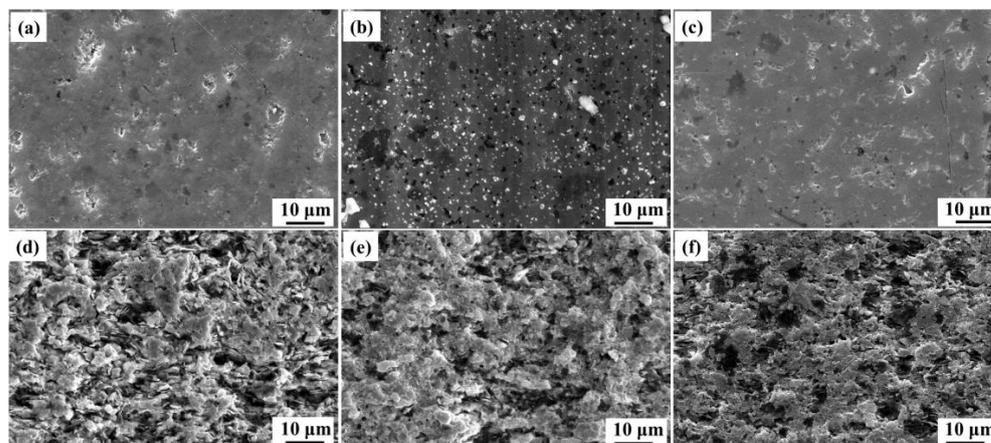

Figure 9. A layer (**a**) and B layer (**d**) of Al_2O_3/graphite-Al_2O_3 laminated composites. Worn surfaces under water conditions with SiO_2 particles (**b**,**e**) and without SiO_2 particles (**c**,**f**).

Table 1 shows the atomic percentages of the elements in the lines of the images in Figure 8. Line 1 and line 2 are on the worn surface under the water working condition with SiO_2 particles (Figure 8a), and line 3 and line 4 are on the worn surface under the water condition without SiO_2 particles (Figure 8c). Compared with line 3 on the A layer (the Al_2O_3 phase), the carbon content of line 1 is lower than that in line 3; the main reason is that the graphite lubrication film was worn off. The silicon and oxygen contents of line 1 are higher than those of line 3, which is mainly due to the SiO_2 particles embedded into the friction surface under the working condition with suspended SiO_2 particles. Meanwhile, compared with line 4, the silicon content of line 2 is increased because of the B layer (the graphite-Al_2O_3 composite phase) containing the softer graphite phase that makes SiO_2 abrasive particles emb in the worn surface easily. This is caused by the hardness of the B layer (HV374 $\pm$ 20), which is lower than that of the A layer (HV1408 $\pm$ 85). The embedded SiO_2 particles in the wear surface can also be observed during the friction process in Figure 10; the atomic distribution of Si is higher in the B layer than that in the A layer.

Table 1. Atomic percentages of the elements in the lines of Figure 8.

Line	Elements' Atomic Percentages (%)			
	C	Al	O	Si
1	22.49	42.15	33.36	2.00
2	55.80	15.79	26.54	1.86
3	27.93	41.32	29.75	1.00
4	55.60	18.16	25.93	0.31

The interface steps between the A layer and the B layer of the Al_2O_3/graphite-Al_2O_3 laminated composites were observed, and the depths of the wear track of the laminated composites perpendicular to the layer direction were studied. In Figure 11a, it can be seen that the worn surface of the laminated composites is not continuous and has obvious furrows and peeling under the water working condition with SiO_2 particles. The wear and tear of the graphite-Al_2O_3 composites (the B layer) are higher than those of the Al_2O_3 ceramic (the A layer), especially in the middle of the sliding distance. The maximum depth of the wear track for the graphite-Al_2O_3 composites (the B layer) is 18.48 $\pm$ 6.77 µm, and

the maximum depth of the wear track for the Al_2O_3 ceramic (the A layer) is 6.28 ± 0.87 μm. This indicates that the friction surface is uneven and that the graphite falls off unevenly. For the worn track of the laminated composites under the water working condition without SiO_2 particles, the wear and tear of the A layer and the B layer are different. The frictional behavior under the water working conditions is similar to polishing with water; the specimen surface becomes smoother, the roughness decreases, and the friction coefficient decreases as well. The maximum depth of the wear track of the graphite-Al_2O_3 composite layer (the B layer) is 6.06 ± 1.56 μm, and the maximum depth of the wear track of the Al_2O_3 ceramic layer (the A layer) is 4.27 ± 0.18 μm. The wear of the A layer is not severe because the Al_2O_3 has a high hardness. The wear mode of the B layer (the graphite-Al_2O_3 composites) under the water working condition without SiO_2 particles is mainly dominated by water lubrication and spalling accompanied by slight abrasive wear, while it is mainly dominated by abrasive wear and evident furrowing presents itself under the water working condition with SiO_2 particles.
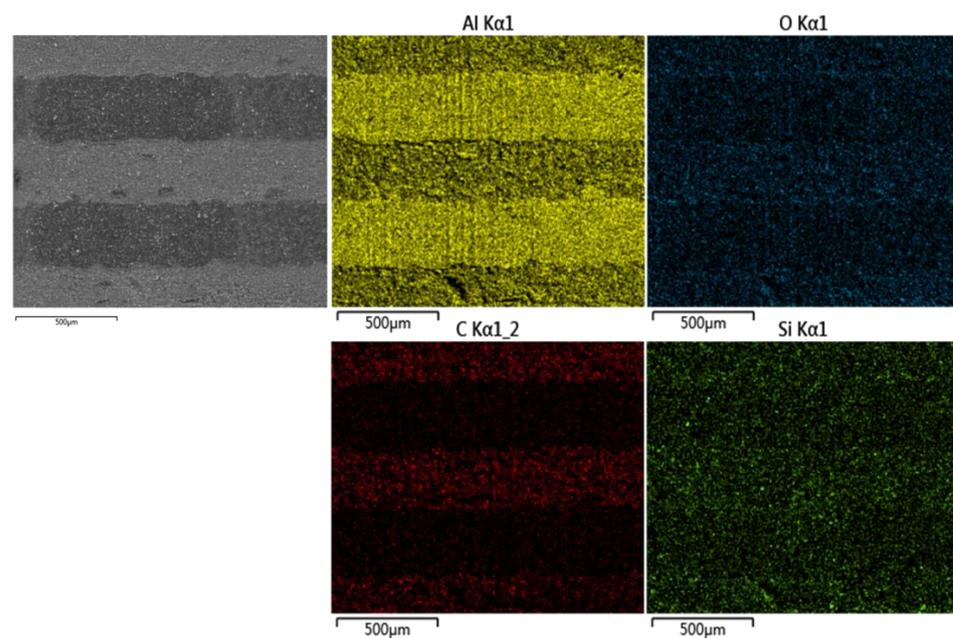

Figure 10. EDS mapping of Al_2O_3/graphite-Al_2O_3 laminated composites under water working condition with SiO_2 particles.
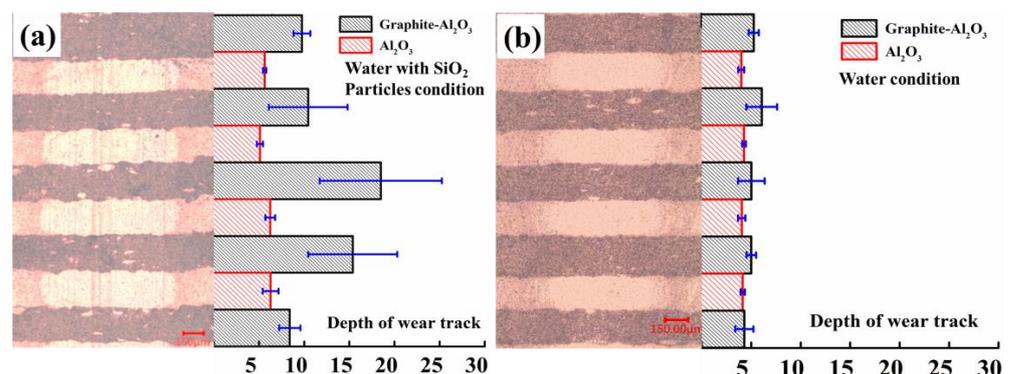

Figure 11. The depth of the wear track of the Al_2O_3/graphite-Al_2O_3 laminated composites under water working conditions with (**a**) and without (**b**) SiO_2 particles.

In short, under water working conditions, the formation of water-lubricating film, the water absorption and expansion of graphite, and the erosion of wear debris from water improve the anti-wear properties of layered materials. However, under conditions with

SiO_2 suspended particles, the solid particles will destroy the lubricating film during friction, which is unfavorable for the reduction in friction and wear. Finally, the addition of graphite can decrease the frictional resistance of laminated Al_2O_3/graphite-Al_2O_3 composites, but its wear rate strongly depends on the working conditions.

4. Conclusions

The tribological performance of the Al_2O_3/graphite-Al_2O_3 laminated composite under water lubrication conditions has been studied in the present work. The results are useful for optimizing and designing sealing devices under water working conditions and improving their service lives. The conclusions drawn are as follows:

(1) The surface of the Al_2O_3/graphite-Al_2O_3 laminated composite perpendicular to the layer direction shows excellent tribological properties under dry friction, water working conditions, and the water condition with SiO_2 suspended particles. The friction coefficient and the wear rate can be as low as 0.16 and 1.76×10^{-6} mm^3/Nm, respectively, under water lubrication, which values are better than those of graphite-Al_2O_3 composites and Al_2O_3/graphite laminated composites.

(2) In the water working conditions, the water-lubricating film and the graphite film separate the contact surfaces and improve the anti-wear properties of the layered structure. However, when SiO_2 particles are added into the water, they destroy the graphite lubricating film, aggravating the friction and wear slightly.

(3) The abrasive wear dominates the wear mode of alumina in the laminated Al_2O_3/graphite-Al_2O_3 composite, while for the graphite in the composite, the wear mode is mainly dominated by the adhesion wear.

Author Contributions: Methodology, H.F.; Validation, Y.S.; Formal analysis, J.S. (Junjie Song); Investigation, J.S. (Jiaxin Si); Resources, Z.W.; Data curation, X.Z.; Writing—original draft, Z.D.; Supervision, L.H. and Y.Z. All authors have read and agreed to the published version of the manuscript.

Data Availability Statement: Data available on request from the authors.

Conflicts of Interest: The authors declare no conflict of interest.

References

1. Wang, Z.; Fan, J.; Zhang, B. Failure analysis of the aircraft accessories graphite seal ring. *IOP Conf. Ser. Earth Environ. Sci.* **2021**, *781*, 022059. [CrossRef]
2. Andersson, S.; Söderberg, A.; Björklund, S. Friction models for sliding dry, boundary and mixed lubricated contacts. *Tribol. Int.* **2007**, *40*, 580–587. [CrossRef]
3. Carrapichano, J.M.; Gomes, J.R.; Oliveira, F.J.; Silva, R.F. Si_3N_4 and Si_3N_4/SiC composite rings for dynamic sealing of circulating fluids. *Wear* **2003**, *255*, 695–698. [CrossRef]
4. Déprez, P.; Hivart, P.; Coutouly, J.F.; Debarre, E. Friction and wear studies using Taguchi method: Application to the characterization of carbon-silicon carbide tribological couples of automotive water pump seals. *Adv. Mater. Sci. Eng.* **2009**, *2009*, 830476. [CrossRef]
5. Blau, P.J.; Dumont, B.; Braski, D.N.; Jenkins, T.; Zanoria, E.S.; Long, M.C. Reciprocating friction and wear behavior of a ceramic-matrix graphite composite for possible use in diesel engine valve guides. *Wear* **1999**, *225–229*, 1338–1349. [CrossRef]
6. Sliney, H.E. Rare earth fluorides and oxides—An exploratory study of their use as solid lubricants at temperatures to 1000 °C. *NASA TN* **1969**, *D-5301*, 190–200.
7. Li, A.; Chen, Q.; Wu, G.; Wang, Y.; Lu, Z.; Zhang, G. Probing the lubrication mechanism of multilayered Si-DLC coatings in water and air environments. *Diam. Relat. Mater.* **2020**, *105*, 107772. [CrossRef]
8. Zhang, Y.-Y.; Chen, Q.; Mo, X.-L.; Huang, P.; Li, Y.-Q.; Zhu, C.-C.; Hu, N.; Fu, S.-Y. Tribological behavior of short carbon fiber reinforced polyetherimide composite under water lubrication conditions. *Compos. Sci. Technol.* **2021**, *216*, 109044. [CrossRef]
9. Zum Gahr, K.H.; Mathieu, M.; Brylka, B. Friction control by surface engineering of ceramic sliding pairs in water. *Wear* **2007**, *263*, 920–929. [CrossRef]

10. Gupta, A.; Pattnayak, A.; Abhijith, N.V.; Kumar, D.; Chaudhry, V.; Mohan, S. Development of alumina-based hybrid composite coatings for high temperature erosive and corrosive environments. *Ceram. Int.* **2023**, *49*, 862–874. [CrossRef]

11. Su, Y.; Zhang, Y.; Song, J.; Hu, L. Novel approach to the fabrication of an alumina-MoS$_2$ Self-lubricating composite via the in situ synthesis of nanosized MoS$_2$. *ACS Appl. Mater. Interfaces* **2017**, *9*, 30263–30266. [CrossRef]

12. Qi, Y.-E.; Zhang, Y.-S.; Hu, L.-T. High-temperature self-lubricated properties of Al$_2$O$_3$/Mo laminated composites. *Wear* **2012**, *280–281*, 1–4. [CrossRef]

13. Song, J.; Zhang, Y.; Fan, H.; Hu, T.; Hu, L.; Qu, J. Design of interfaces for optimal mechanical properties in Al$_2$O$_3$/Mo laminated composites. *J. Eur. Ceram. Soc.* **2015**, *35*, 1123–1127. [CrossRef]

14. Zhang, Y.; Su, Y.; Yuan, F.; Qi, Y.; Hu, L. High-performance self-lubricating ceramic composites with laminated-graded structure. In *Advances in Functionally Graded Materials and Structures*; IntechOpen: London, UK, 2016.

15. Song, J.; Zhang, Y.; Fang, Y.; Fan, H.; Hu, L.; Qu, J. Influence of structural parameters and transition interface on the fracture property of Al$_2$O$_3$/Mo laminated composites. *J. Eur. Ceram. Soc.* **2015**, *35*, 1581–1591. [CrossRef]

16. Song, J.; Zhang, Y.; Su, Y.; Fang, Y.; Hu, L. Influence of structural parameters and compositions on the tribological properties of alumina/graphite laminated composites. *Wear* **2015**, *338–339*, 351–361. [CrossRef]

17. Song, J.; Yang, H.; Bermejo, R.; Qu, J.; Hu, L.; Zhang, Y. Enhanced thermal shock response of Al$_2$O$_3$–graphite composites through a layered architectural design. *J. Am. Ceram. Soc.* **2019**, *102*, 3673–3684. [CrossRef]

18. Strey, N.F.; Ramos, R.; Scandian, C. Superlubricity and running-in wear maps of water-lubricated dissimilar ceramics. *Wear* **2022**, *498–499*, 204328. [CrossRef]

19. Kalin, M.; Novak, S.; Vižintin, J. Surface charge as a new concept for boundary lubrication of ceramics with water. *J. Phys. D Appl. Phys.* **2006**, *39*, 3138. [CrossRef]

20. Jia, J.-H.; Chen, J.-M.; Zhou, H.-D.; Wang, J.-B.; Zhou, H. Friction and wear properties of bronze–graphite composite under water lubrication. *Tribol. Int.* **2004**, *37*, 423–429. [CrossRef]

21. Zhao, W.; Zhang, G.; Dong, G. Friction and wear behavior of different seal materials under water-lubricated conditions. *Friction* **2021**, *9*, 697–709. [CrossRef]

22. Xie, Z.; Zhang, Y.; Zhou, J.; Zhu, W. Theoretical and experimental research on the micro interface lubrication regime of water lubricated bearing. *Mech. Syst. Signal Process.* **2021**, *151*, 107422. [CrossRef]

23. Liu, H.; Xue, Q. The tribological properties of TZP-graphite self-lubricating ceramics. *Wear* **1996**, *198*, 143–149. [CrossRef]

24. Hass, K.C.; Schneider, W.F.; Curioni, A.; Andreoni, W. The chemistry of water on alumina surfaces: Reaction dynamics from first principles. *Science* **1998**, *282*, 265–268. [CrossRef] [PubMed]

25. Zhang, H.; Hu, X.; Yan, J.; Tang, S. Study of wear behavior of MoSi$_2$ under water lubrication. *Mater. Lett.* **2005**, *59*, 583–587. [CrossRef]

26. Wu, J.; Cheng, X.H. The tribological properties of Kevlar pulp reinforced epoxy composites under dry sliding and water lubricated condition. *Wear* **2006**, *261*, 1293–1297. [CrossRef]

27. Di Maro, M.; Duraccio, D.; Malucelli, G.; Faga, M.G. High density polyethylene composites containing alumina-toughened zirconia particles: Mechanical and tribological behavior. *Compos. Part B Eng.* **2021**, *217*, 108892. [CrossRef]

28. Kozbial, A.; Zhou, F.; Li, Z.; Liu, H.; Li, L. Are graphitic surfaces hydrophobic? *Acc. Chem. Res.* **2016**, *49*, 2765–2773. [CrossRef]

29. Picaud, S.; Collignon, B.; Hoang, P.N.M.; Rayez, J.C. Molecular dynamics simulation study of water adsorption on hydroxylated graphite surfaces. *J. Phys. Chem. B* **2006**, *110*, 8398–8408. [CrossRef]

30. Chen, L.; Qian, L. Role of interfacial water in adhesion, friction, and wear—A critical review. *Friction* **2021**, *9*, 1–28. [CrossRef]

31. Guo, F.; Tian, Y.; Liu, Y.; Wang, Y. Ultralow friction between cemented carbide and graphite in water using three-step ring-on-ring friction test. *Wear* **2016**, *352–353*, 54–64. [CrossRef]